Chapter 7

Design of Experiment Approach in the Industrial Gas Carburizing Process

Muhammad Atiq Ur Rehman,
Muhammad Azeem Munawar, Qaisar Nawaz and
Muhammad Yousaf Anwar

Additional information is available at the end of the chapter

http://dx.doi.org/10.5772/intechopen.72822

Abstract

Carburized samples were prepared under different sets of conditions at Millat Equipment Limited, Lahore, Pakistan, using continuous carburizing furnace under a reducing atmosphere. The gas carburizing process parameters were determined by the Taguchi design of experiment (DoE), an orthogonal array of L9 type with the mixed level of control factors. The key process parameters in gas carburizing process such as delay quenching interval, hardening temperature, and soaking time in oil were optimized in terms of core hardness, effective case depth (ECD), and surface hardness. DoE approach elucidated that the best results in terms of core hardness are A2 (delay quenching for 60 seconds), B2 (hardening temperature of 800°C), and C2 (soaking in quenching oil for 300 seconds). However, the best results in terms of ECD were A1 (delay quenching for 45 seconds), B3 (hardening temperature of 820°C), and C1 (soaking in quenching oil for 180 seconds). In order to choose the optimized parameters from the results given by DoE, microscopic analysis was conducted. Microscopic analysis showed coarse bainitic structure in core and tempered martensite at the surface of the samples processed at A2 (delay quenching for 60 seconds), B2 (hardening temperature of 800°C), and C1 (soaking in quenching oil for 180 seconds) compared to the other process conditions (A1, B3, and C1), which shows fine bainitic structure at core and relatively higher amount of retained austenite at the surface. Finally, defect per million opportunities (DPMO) model exhibited that the samples produced from the optimized set of parameters (A2, B2, and C1) are highly reproducible, gaining DPMO of 83 parts per million (PPM).

Keywords: gas carburizing, core hardness, design of experiment, defect per million opportunities, effective case depth

1. Introduction

In the current era, most of the industries are focusing on economical process optimization techniques. The most common industrial approaches are trial-and-error approach or one variable at a time (OVAT) in which one variable is changed at one time [1, 2]. These approaches are inefficient and time-consuming. However, statistical tools, such as the Taguchi design of experiments (DoE), provide superior methods to conduct experiments by efficient means. The selection of investigated parameters involved in the process is based on the philosophy of Dorian Shainin, which is characterized by focusing on a limited number of parameters selected by their cause and effect relationship [2, 3]. Hence, the Taguchi DoE has been widely used nowadays in the industrial sector. Moreover, Taguchi DoE approach allows changing more than one factor at one time, which reduces the number of experiments required to determine the optimized parameter [2, 4–6].

The Taguchi DoE assesses the effect and significance of controllable factors of an experiment, which increases the robustness of a process. Robustness is measured as a signal-to-noise (S/N) ratio. It comprises the sensitivity of the signal to disturbing factors involved in the process, the so-called noise [4, 7]. The optimization process is based on the assessment of this ratio as it determines the impact of control factors on the process. The DoE provides an efficient method for the optimization since only a limited number of experiments are required in contrast to full factorial methods [3, 8–10]. The statistical significance of each control factor can be determined by the performance of the multivariate analysis of variance (MANOVA). The significance of individual control factors can be estimated by its probability value p [5, 7].

Another important factor in the industrial process is the reproducibility. Design of experiment approach can further help in improving the reproducibility of the process. An important method to determine the reproducibility of the process is defect per million opportunities model (DPMO). DPMO evaluates the reproducibility of the process to relatively high sensitivity such as parts per million (PPM) [11, 12]. The “Six Sigma” approach can help in achieving the highly reproducibility of the industrial process. Therefore, it can be concluded that DoE approach coupled with the Six Sigma can help in economical process optimization at higher statistical confidence and reproducibility. Finally, KAIZEN “tools for continuous improvement” can help in sustaining the optimized experimental conditions [12].

Taguchi DoE is applied here to solve the particular industrial problems related with the higher field failure rate of crown wheel pinion. For example, field failure for the pinion after only 200 working hours was taken into account. Microscopic examination of sectioned piece revealed Chevron nature of fracture. Metallographic studies were also taken into account to know the reason behind this premature failure. Findings were the higher value of core hardness (38 HRC), with 25% of retained austenite. In service the retained austenite, which is metastable phase, will transform into martensite raising brittleness, because newly formed martensite is untempered. In addition, this newly formed martensite will cause dimensional changes as well as cause unexpected shift of contact pattern and backlash of more than 0.01 mm. Higher value of core hardness will make the core to respond to any sudden shock with minimum absorptivity and maximum transmissibility [13–15]. Furthermore, literature was studied to investigate the reasons behind the higher values of core hardness and retained

austenite. It was found that high quenching temperatures, high quenching oil's temperature, improper diffusion, over carburizing, coarse initial grain size, segregation of the impurities at high-angle grain boundaries, higher value of chromium and silicon, improper soaking in the quenching oil, and viscosity of the oil might also be the reason [16–18]. Higher values of core hardness and retained austenite cause increase in the surface brittleness and improper load distribution behavior under dynamic loading conditions. It is hoped that this research will have paramount importance for industrial development and academic research [17, 19, 20]. Therefore, keeping in view for the criticality of core hardness, it was aimed to develop an intermediate and compromised value of core hardness during the carburizing process. In this research work, we choose delay quenching time, soaking time in oil, and hardening temperature as the significant parameters on the basis of fishbone diagram. Afterward, the effect of each parameter at various levels was studied to determine the optimum gas carburizing conditions.

2. Materials and methods

2.1. Materials

The material used in the present experimental work was a low-carbon low-alloy steel (SAE 8620). The chemical composition of the steel is given in **Table 1**.

The addition of alloying elements such as Mn, Mo, Ni, and Cr increases the hardening ability of the steel. The depth to which the steel is hardened is usually called as the hardenability of the steel.

2.2. Gas carburizing process

Test coupons were made up of 8620 low-alloy steel having dimensions of 2 × 1 (inch^2). One of the test samples was subjected to destructive testing for the metallography (microstructure

Element	Composition (mol %)
C	0.18–0.23
Si	0.15–0.35
Mn	0.7–0.9
Mo	0.150–0.25
S	0.04 max
P	0.35 max
Ni	0.4–0.7
Cr	0.4–0.6

Table 1. Chemical composition for 8620 alloy steel determined by using spark arc emission spectroscopy at AFCO Steel Mills Pvt Ltd., Lahore, Pakistan.

is shown in **Figure 5(D)**). Hardness was measured for all the samples prior to carburizing (150–200 HB, Brinell hardness number). Samples were charged into the continuous carburizing furnace (Gibbons furnace, UK) having fixed carburizing time (3.5 hours), carburizing temperature (930°C), and carbon potentials (1.00), but varying quenching time, holding in air (delay quenching intervals) before quenching, and hardening temperatures. It is important to highlight that carburizing time, carburizing temperature, and carbon potential were determined from the fishbone diagram (data not shown here), following previous studies [7, 10, 21]. Endo-gas (CO) was provided from endothermic gas generator to maintain reducing environment in the furnace. Diffusion of carbon took place in the same furnace but at comparatively low temperatures (780–840°C) and low values of flow rates of enrichment gas than in the carburizing process. Quenching was done in quenching tank of 12 × 10 × 8 feet at 75°C. Samples were tempered in the conveyer type tempering furnace at 120°C; prior to this washing was done.

2.3. Metallography

Metallography consists of studying the microscopic structure and characteristics of a given metal or an alloy. Metallography determines grain size, grain shape distribution of various phases and inclusions, and mechanical and thermal treatment of metals [22]. The non heat treated samples were sectioned using manual hacksaw whereas for cutting the heat treated samples abrasive cutoff wheel was used [22, 23].

Samples were cut and machined into 1 × 2 ($inch^2$) for the carburizing process, as shown in **Figure 1**. Test coupons after the gas carburizing process were subjected to the destructive testing such as effective case depth measurement and microstructural analysis. Prior to these samples were grind and polished (**Figure 2**). Two percent of nital was used to etch (to reveal the internal microstructure) the samples followed by washing with ethyl alcohol and subsequent

Figure 1. Optical image of the machine test coupon used for the carburizing process.

http://dx.doi.org/10.5772/intechopen.72822

Figure 2. Digital image of the mounted samples after cutting, grinding, and polishing showing a mirror-like surface.

drying [22]. Etchant attacks the particles at high energy levels, since grain boundaries are at higher energy level so they become visible under microscope. The microstructure was evaluated at the surface and core with LECO microscope at MEL Quality Assurance Department (microstructures after heat treatment are shown in **Figure 5(A–C)**).

2.4. Effective case depth (ECD) measurement

ECD was measured with "Micro Vickers Hardness Testing Machine" (Shimadzu, Japan). Polished samples were placed on the platform, and then harness was measured by the indent steps at 0.1 mm. After taking an indent, mean diagonal length was measured and converted into Vickers pyramid hardness number (VPN). Similar indents were taken at increasing distance till the hardness value of 500 VPN. The distance from surface at which 500 VPN is achieved is known as effective case depth (ECD) [22]. Core hardness was also measured by taking an indent at the center point of test sample.

2.5. Hardness testing

After carburizing samples were subjected to surface hardness test using Rockwell hardness tester in which the first minor load (10 Kg_f) was applied followed by the major load of 300 Kg_f.

2.6. Design of experiments

In order to optimize the gas carburizing of SAE 8620 alloy steel, the basic tools of Six Sigma were applied. Vital parameters offered by the basic diffusion model was scrutinized by cause and effect diagram in terms of intended application (hard case and tough core), which offered the basis for selection of control factors (soaking time in oil, delay quenching interval, and hardening time), as shown in **Table 2**. In order to study the effect of these control factors, an orthogonal array of L9 (three control factors and three levels of each) type with the mixed level of control factors was applied (**Table 3**). The DoE approach was helpful in reducing the number of experiment from 27 (full factorial design) to 9 (DoE array of L9 type). Thus, the optimized parameters can be determined with the less number of experiments.

Symbol	Control factor	Levels		
		1	2	3
A	Delay quenching interval (S)	45	60	90
B	Hardening temperature (°C)	780	800	820
C	Soaking time in oil (S)	180	300	420

Table 2. Control factors and level of variables.

Run	Control factors			Core hardness (HRC)	ECD (mm)	Surface hardness (HRC)	S/N ratio for core hardness (dB)
	Delay quenching interval (S)	Hardening temperature (°C)	Soaking time in oil (S)				
1	45	780	180	26	0.90	57	28,299
2	45	800	300	29	1.00	59	29,248
3	45	820	420	34	1.20	60	30,629
4	60	780	300	22	0.65	58	26,848
5	60	800	420	25	0.80	57	27,958
6	60	820	180	28	0.90	58	28,943
7	90	780	420	20	0.45	56	26,020
8	90	800	180	23	0.60	57	27,234
9	90	820	300	26	0.70	57	28,299

Table 3. Experimentally measured values of core hardness, ECD, and surface hardness for gas carburizing process of SAE 8620 steel.

3. Results and discussion

3.1. Gas carburizing process

In the gas carburizing process, first the test coupons were preheated at 400°C for 30 minutes to avoid thermal shocks. Second, the temperature was raised to 930°C under a reducing environment, which was produced by the flow of CO in the furnace from endothermic gas generator. Moreover, methane gas was enriched in the furnace to maintain the carbon potential of 1.0. At 930°C the solubility of carbon in steel is approximately 1.14 (because steel transforms to the austenitic phase), due to which carbon started to flow from the atmosphere to the samples [18, 24, 25]. After soaking the samples for optimized time period, the surface carbon contents of the samples were raised. Afterward, samples entered into the hardening zone/diffusion zone, where the samples were kept for 1 hour in the temperature range of 780–820°C under a reducing environment [26, 27]. Since the temperature of the samples are dropped now, carbon from the outer surface starts to diffuse into the core [28]. The reason could be that outer

surface is at lower temperature in comparison to that of inner surface of the sample; thus, the solubility of inner portion is reasonably high, which allows the diffusion of carbon [25, 29]. Finally, samples were quenched in the mineral oil at 75°C. The quenching process allows the diffusionless martensitic transformation at the surface [30–32]. However, thermal gradient at the core of the sample is significantly less, which allows the bainitic or ferritic transformation to occur in the core of the samples [32, 33]. The carburizing cycle of the test coupons is shown in **Figure 3**.

3.2. Design of experiment approach for gas carburizing of SAE 8620 steel

Control factors and their levels used in the design of experiment approach are illustrated in **Table 2**.

After the selection of control factors with the help of a cause and effect diagram (not given here), a signal-to-noise ratio (S/N) was calculated for the average core hardness of the heat-treated samples by considering that high value of S/N is desired [4]:

$$\frac{S}{N} = -10\, log\left[\frac{1}{n}\left(\frac{1}{\sum_i^2 Y}\right)\right] \tag{1}$$

where

Y_i is the average core hardness.

n the number of observations.

Unit for S/N ratio is dB.

The design of experiment technique allows studying the effects of each parameter at different levels by averaging S/N ratio at each level. For example, the mean S/N ratio for deposition yield at levels 1, 2, and 3 of control factor A (delay quenching interval) can be calculated by

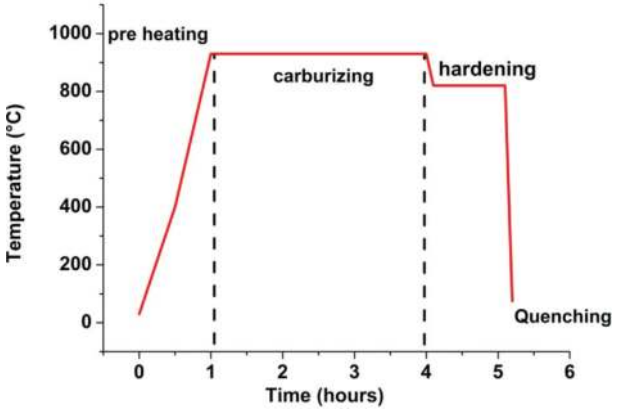

Figure 3. Typical carburizing cycle of the Gibbons furnace for SAE 8620 test coupons.

averaging S/N ratios for experiments 1–3, 4–6, and 7–9, respectively [4, 5, 7]. This technique was used for calculating the response of core hardness and ECD as presented in **Table 3**.

DoE approach was conducted to find out the suitable combination of gas carburizing parameters in order to ensure the optimum gas carburizing parameters with relatively higher statistical confidence. The effect of each control factor on the core hardness and ECD is shown in **Figure 4**, which shows that the parameters, that is, delay quenching interval and hardening temperature, have significant effect on core hardness and case depth. This effect was further confirmed by calculating maximum-minimum values reported in **Tables 4–7**.

Figure 4(A) shows that the increase in delay quenching significantly reduces the core hardness. The increase in hardening temperature tends to increase the core hardness. However, the increased soaking time in oil slightly raises the core hardness value. The aim was to obtain an intermediate value of core hardness; thus, the core should neither be too hard to cause fracture nor too soft to cause core crushing [10, 17, 34]. The intermediate values for the core hardness were attained at A2 (delay quenching interval of 60 seconds), B2 (hardening temperature of 800°C), and C2 (soaking time in oil for 300 seconds) conditions, as shown in **Table 8**. The reason for the decrease in the core hardness with the rise in delay quenching intervals could be the slow cooling of core in air compared to that of oil, which may have led to ferritic

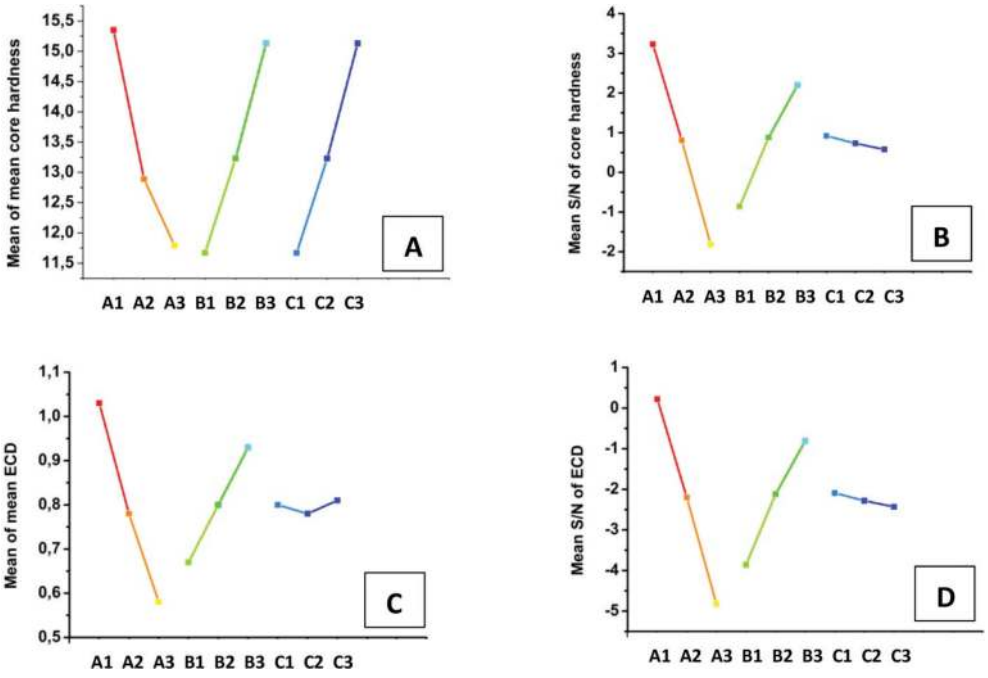

Figure 4. (A) Mean of mean core hardness response of control factors on core hardness, (B) mean of S/N (dB) response for the effect of control factors on core hardness, (C) mean of mean response for the effect of control factors on ECD, and (D) mean of S/N (dB) response for the effect of control factors on ECD.

Level	Delay quenching interval (S)	Hardening temperature (°C)	Soaking time in oil (S)
1	15.35	11.67	13.23
2	12.89	13.23	13.23
3	11.79	15.13	13.58
Maximum-minimum	3.56	3.47	0.35
Rank	1	2	3

Table 4. Mean response for the core hardness.

Level	Delay quenching interval (S)	Hardening temperature (°C)	Soaking time in oil (S)
1	3.23	−0.86	0.92
2	0.81	0.88	0.73
3	−1.82	2.20	0.58
Maximum-minimum	5.04	3.05	3.41
Rank	1	2	3

Table 5. S/N (dB) response for the core hardness.

Level	Delay quenching interval (S)	Hardening temperature (°C)	Soaking time in oil (S)
1	1.03	0.67	0.80
2	0.78	0.80	0.78
3	0.58	0.93	0.81
Maximum-minimum	0.45	0.27	0.03
Rank	1	2	3

Table 6. Mean response for ECD.

Level	Delay quenching interval (S)	Hardening temperature (°C)	Soaking time in oil (S)
1	0.22	−3.86	−2.09
2	−2.20	−2.12	−2.28
3	−4.82	−0.81	−2.43
Maximum-minimum	5.05	3.05	0.34
Rank	1	2	3

Table 7. S/N (dB) response for ECD.

	Delay quenching interval (S)	Hardening temperature (°C)	Soaking time in oil (S)
Optimum parameters for the best ECD	45 (A1)	820 (B3)	180 (C1)
Optimum parameters for the best core hardness	60 (A2)	800 (B2)	300 (C2)
Optimum parameters for the best combination of ECD, core hardness, and microstructure	60 (A2)	800 (B2)	180 (C1)

Table 8. Illustration of the best possible condition for optimum ECD, core hardness, and the combination of core hardness, ECD, and microstructure.

transformation at core rather than the bainitic transformation [21, 30], thus lowering the core hardness values of the specimens. Similar effect may be held responsible for the drop in core hardness values with the decrease in immersion time in oil [22].

Figure 4(C) shows the effect of control factors on the effective case depth. Here, the maximum value of case depth is required to provide high wear resistance for longer period of time [33]. The most significant parameter was the delay quenching interval. Reducing the delay time significantly improves the ECD, which may be due to the fact that rapid quenching hinders the diffusion of carbon toward the core of the sample. Thus, we formed uniform and shallow case depth during the hardening process. It was inferred from **Figure 4(C** and **D)** that best parameters in terms of the ECD are A1 (delay quenching of 45 seconds), B3 (hardening temperature of 820°C), and C1 (soaking in oil for 180 seconds).

It was concluded that there is a contrast in the best results for ECD and core hardness. Therefore, it was essential to establish a trade-off between the ECD and core hardness. Thus, we choose A2 (delay quenching of 60 seconds), B2 (hardening temperature of 800°C), and C1 (soaking in oil for 180 seconds), as the best condition. Soaking time in oil was the least significant factor; thus, it was chosen on the basis of the highest possible case depth. On the other hand, A2 and B2 were selected on the basis of core hardness because it was established in our previous studies that hard core will cause the premature failure of the components. Moreover, the microstructural analysis of the samples hardened at 820°C shows the formation of relatively higher amount of retained austenite (almost 25%, as shown in **Figure 5(A)**), which is a brittle phase and may also undergo dimensional changes, because retained austenite will eventually transform into the martensite in service [17, 19, 30]. It is important to highlight that the quantitative analysis was done with the software equipped with the LECO microscope, which quantitatively gives the amount of each phase present in the microstructure. Dimensional changes during the operation/service are deleterious, which may result in uneven load distribution between the matting parts. For example, the field failure investigations of different components show the deviations in pitch circle diameter (PCD), face runout (FR), and backlash (BL) level for the components with relatively higher amount of retained (higher amounts of retained austenite led to the dimensional changes in the components during the service).

On the other hand, samples processed at optimized conditions (A2, B2, and C1) showed a coarse bainitic structure (**Figure 5(B)**), which is considered as one of the toughest structures of steel [22, 23]. Moreover, the surface of the sample was covered with tempered martensite, as shown in **Figure 5(C)**.

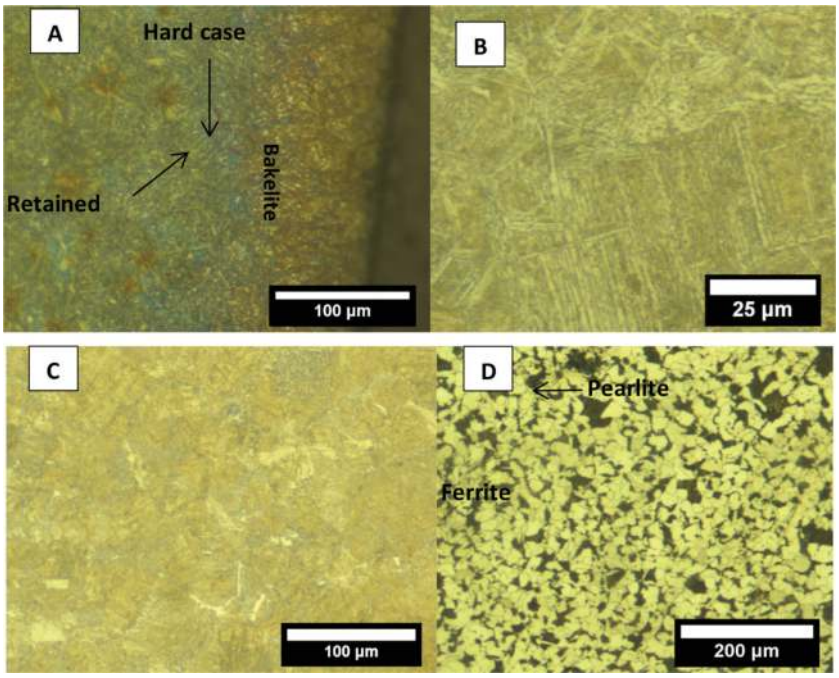

Figure 5. Optical microscope images of the samples: (A) microstructure of the sample processed at A1, B3, and C1 conditions; (B) microstructure at the core of the sample processed at A2, B2, and C1 conditions; (C) microstructure at the surface of the sample processed at A2, B2, and C1 conditions; and (D) microstructure of the SAE 8620 low-alloy steel prior to the carburizing.

Figure 5(D) shows the microstructure of the SAE 8620 alloy steel prior to the heat treatment. It was observed that the microstructure is comprised up of fine grains with relatively higher amount of pearlite dispersed with small amount of ferrite as well, as shown in **Figure 5(D)**. Thus, it can be concluded that the microstructure of the specimen is in the suitable range for the heat treatment process. In the present study, the grain size was measured by using ASTM standards whereas the amounts of ferrite (10%) and pearlite (90%) in the sample were analyzed by using the software equipped with LECO microscope.

3.3. Defect per million opportunities (DPMO) model

In order to gain deep insight of the optimized parameters predicted by the DoE array, DPMO was calculated by using the following formula [12]:

$$DPMO = \frac{no.\ of\ defects\ found\ in\ a\ sample}{sample\ size \times no.\ of\ defect\ opportunities\ per\ unit} \times 10{,}00{,}000 \quad (2)$$

A number of defect opportunities were 24, which could be calculated by the help of cause and effect diagram (not reported here). In short, the cause and effect diagram takes into account both internal (environment, human error, machine error, machine constraints, etc.) and external factors (carburizing time, carburizing temperature, carbon potential, hardening time, etc.).

However, at least 10,000 experiments were conducted from the optimized set of parameters, that is, A2, B2, and C1, but no significant variations were observed. This may be due to the fact that DoE approach takes into account almost all factors at the same time. Thus, the chances for the deviations are minimized. DPMO for the optimized set of conditions was 83, which is quite good according to the Six Sigma approach. Moreover, considering the complexity of the gas carburizing process, it must be highlighted that achieving such a high reproducibility of the surface treatment process is a challenging task, which was accomplished by the DoE approach. The present study is believed to be helpful in further reducing the DPMO values upon further improvements in this study.

4. Conclusions

The conclusions of this chapter are listed as follows:

1. SAE 8620 low-alloy steel was successfully case hardened under various conditions.
2. Control parameters and their levels for the gas carburizing process were selected on the basis of fishbone diagram.
3. Taguchi design of experiment approach was applied to build L9 matrix.
4. Control parameters and their levels were studied in terms of ECD, core hardness, and surface hardness.
5. DoE approach elucidated that the best parameters are delay quenching interval of 60 seconds, hardening temperature of 800°C, and soaking time in oil for 180 seconds.
6. The samples processed at optimized parameters possessed coarse bainitic structure at core and tempered martensite at the surface.
7. The optimized parameters were highly reproducible, as evaluated by the DPMO model.

Author details

Muhammad Atiq Ur Rehman[1,4], Muhammad Azeem Munawar[2], Qaisar Nawaz[3] and Muhammad Yousaf Anwar[4]*

*Address all correspondence to: myanwar@uet.edu.pk

1 Institute of Space Technology Islamabad, Islamabad, Pakistan

2 Institute of Polymer Materials Friedrich-Alexander – University, Erlangen-Nuremberg, Erlangen, Germany

3 Department of Material Science and Engineering, Institute of Biomaterials, University of Erlangen Nuremberg, Erlangen, Germany

4 Department of Metallurgical and Materials Engineering, University of Engineering and Technology Lahore, Lahore, Pakistan

References

[1] Murugan VK, Mathews PK. Optimization of heat treatment processes using Taguchi's parameter design approach. International Journal of Research in Mechanical Engineering. 2013;**1**:16-21. ISSN Online: 2347-5188 Print: 2347-8772

[2] Tsui KL. An overview of Taguchi method and newly developed statistical methods for robust design. IIE Transaction on Institute Industrial Engineering. 1992;**24**:44-57. DOI: 10.1080/07408179208964244

[3] Rao RS, Kumar CG, Prakasham RS, Hobbs PJ. The Taguchi methodology as a statistical tool for biotechnological applications: A critical appraisal. Biotechnology Journal. 2008;**3**:510-523. DOI: 10.1002/biot.200700201

[4] Atiq Ur Rehman M, Bastan FE, Haider B, Boccaccini AR. Electrophoretic deposition of PEEK/bioactive glass composite coatings for orthopedic implants: A design of experiment (DoE) study. Materials and Design. 2017;**130**:223-230. DOI: 10.1016/j.matdes.2017.05.045

[5] Pishbin F, Simchi A, Ryan MP, Boccaccini AR. A study of the electrophoretic deposition of bioglass® suspensions using the Taguchi experimental design approach. Journal of the European Ceramic Society. 2010;**30**:2963-2970. DOI: 10.1016/j.jeurceramsoc.2010.03.004

[6] Corni I, Cannio M, Romagnoli M, Boccaccini AR. Application of a neural network approach to the electrophoretic deposition of PEEK–alumina composite coatings. Materials Research Bulletin. 2009;**44**:1494-1501. DOI: 10.1016/j.materresbull.2009.02.011

[7] Fatoba OS, Akanji OL, Aasa AS. Optimization of carburized UNS G10170 steel process parameters using Taguchi approach and response surface model (RSM). Journal of Minerals and Materials Characterization and Engineering. 2014;**02**:566-578

[8] Karabelchtchikova O. Fundamentals of mass transfer in gas carburizing [PhD thesis]. Worcester, USA: Worcester Polytechnic Institute; 2007

[9] Pishbin F, Simchi A, Ryan MP, Boccaccini AR. Electrophoretic deposition of chitosan/45S5 bioglass composite coatings for orthopaedic applications. Surface and Coatings Technology. 2011;**205**:5260-5268. DOI: 10.1016/j.surfcoat.2011.05.026

[10] Kumar S, Rakesh Kumar SA. Optimization of heat treatment processes of steel used in automotive bearings. International Journal of Technical Research & Applications. 2016;**4**:38-44

[11] Gerald JH, Doganaksoy N, Hoerl R. The evolution of six sigma. Quality Engineering Journal. 2000;**12**:317-326. doi.org/10.1080/08982110008962595

[12] Şenvar Ö, Tozan H. Process capability and six sigma methodology including fuzzy and lean approaches. In: Products And Services: From R&D To Final Solutions. Rijeka: Intech, Cop; 2010. pp. 153-178. Available from: http://www.intechopen.com/source/pdfs/12326/InTech-Process_capability_and_six_sigma_methodology_including_fuzzy_and_lean_approaches.pdf

[13] Boniardi M, D'Errico F, Tagliabue C. Influence of carburizing and nitriding on failure of gears – A case study. Engineering Failure Analysis. 2006;**13**:312-339. DOI: 10.1016/j.engfailanal.2005.02.021

[14] Bensely A, Stephen JS, Mohan LD, Nagarajan G, Rajadurai A. Failure investigation of crown wheel and pinion. Engineering Failure Analysis. 2006;**13**:1285-1292. DOI: 10.1016/j.engfailanal.2005.10.002

[15] Sugianto A, Narazaki M, Kogawara M, Shirayori A, Kim SY, Kubota S. Numerical simulation and experimental verification of carburizing-quenching process of SCr420H steel helical gear. Journal of Materials Processing Technology. 2009;**209**:3597-3609. DOI: 10.1016/j.jmatprotec.2008.08.017

[16] Asi O, Can AC, Pineault J, Belassel M. The relationship between case depth and bending fatigue strength of gas carburized SAE 8620 steel. Surface and Coatings Technology. 2007;**201**:5979-5987. DOI: 10.1016/j.surfcoat.2006.11.006

[17] Genel K. Effect of case depth on fatigue performance of AISI 8620 carburized steel. International Journal of Fatigue. 1999;**21**:207-212. DOI: 10.1016/S0142-1123(98)00061-9

[18] Asi O, Can AC, Pineault J, Belassel M. The effect of high temperature gas carburizing on bending fatigue strength of SAE 8620 steel. Materials & Design. 2009;**30**:1792-1797. DOI: 10.1016/j.matdes.2008.07.020

[19] Richman RH, Landgraf RW. Some effects of retained austenite on the fatigue resistance of carburized steel. Metallurgical Transactions A. 1975;**6**:955-964. DOI: 10.1007/BF02661347

[20] Jian-Min T, Yi-Zhong Z, Tian-Yi S, Hai-Jin D. The influence of retained austenite in high chromium cast iron on impact-abrasive wear. Wear. 1990;**135**:217-226. DOI: 10.1016/0043-1648(90)90026-7

[21] Palaniradja K, Alagumurthi N, Soundararajan V. Optimization of process variables in gas carburizing process: A Taguchi study with experimental investigation on SAE 8620 and AISI 3310 steels. Turkish Journal of Engineering and Environmental Sciences. 2005;**29**:279-284

[22] Avner SH. Introduction to Physical Metallurgy. 2nd ed. New York: McGraw Hill; 1974

[23] Callister W, Rethwisch D. Materials Science and Engineering: An Introduction. New York: Wiley; 2007. DOI: 10.1016/0025-5416(87)90343-0

[24] Zhang X, Tang J, Zhang X. An optimized hardness model for carburizing-quenching of low carbon alloy steel. Journal of Central South University. 2017;**24**:9-16. DOI: 10.1007/s11771-017-3403-2

[25] Karabelchtchikova O, Sisson RD. Carbon diffusion in steels: A numerical analysis based on direct integration of the flux. Journal of Phase Equilibria and Diffusion. 2006;**27**:598-604. DOI: 10.1007/BF02736561

[26] Singer F, Kufner M. Model based laser-ultrasound determination of hardness gradients of gas-carburized steel. NDT&E International. 2017;**88**:24-32. DOI: 10.1016/J.NDTEINT.2017.02.006

[27] Smirnov AE, Ryzhova MY, Semenov MY. Choice of boundary condition for solving the diffusion problem in simulation of the process of vacuum carburizing. Metal Science and Heat Treatment. 2017;**59**:237-242. DOI: 10.1007/s11041-017-0135-8

[28] Zhao J, Wang GX, Ye C, Dong Y. A numerical model coupling diffusion and grain growth in nanocrystalline materials. Computational Materials Science. 2017;**136**:243-252. DOI: 10.1016/j.commatsci.2017.05.010

[29] Tao Q, Wang J, Fu L, Chen Z, Shen C, Zhang D. Ultrahigh hardness of carbon steel surface realized by novel solid carburizing with rapid diffusion of carbon nanostructures. Journal of Materials Science and Technology. 2017;**33**:1210-1218. DOI: 10.1016/J.JMST.2017.04.022

[30] Easton D, Perez M. Effects of forming route and heat treatment on the distortion behaviour of case-hardened martensitic steel type S156. In: Heat Treatment. Ohio: At Columbus; 2017

[31] Peng YW, Gong JM, Jiang Y, Fu MH, Rong DS. Influence of plastic pre-strain on low-temperature gas carburization of 316L austenitic stainless steel. Applied Mechanics and Materials. 2016;**853**:178-183. DOI: 10.4028/www.scientific.net/AMM.853.178

[32] Dal'Maz Silva W, Dulcy J, Ghanbaja J, Redjaïmia A, Michel G, Thibault S, Belmonte T. Carbonitriding of low alloy steels: Mechanical and metallurgical responses. Materials Science and Engineering A. 2017;**693**:225-232. DOI: 10.1016/j.msea.2017.03.077

[33] Liew WYH, Ling JLJ, Siambun NJ. Sliding wear behaviour of steel carburized using Na_2CO_3–NaCl. MATEC Web Conferences. 2017;**87**:2010. DOI: 10.1051/matecconf/20178702010

[34] Palaniradja K, Alagumurthi N, Soundararajan V. Hardness and case depth analysis through optimization techniques in surface hardening processes. The Open Materials Science Journal. 2010;**4**:38-63